Journal of Photochemistry and Photobiology A: Chemistry 203 (2009) 7–12

Contents lists available at ScienceDirect

Journal of Photochemistry and Photobiology A: Chemistry

journal homepage: www.elsevier.com/locate/jphotochem

Complexation of Mg-tetrabenzoporphyrin with pyridine enhances singlet oxygen generation and affects its partitioning into apolar microenvironments

Hana Weitman, Smadar Shatz, Benjamin Ehrenberg*,[1]

Department of Physics and Nano Medicine Research Center, Institute of Nanotechnology and Advanced Materials, Bar Ilan University, Ramat Gan, Israel

ARTICLE INFO

Article history:
Received 14 April 2008
Received in revised form
20 November 2008
Accepted 26 November 2008
Available online 20 January 2009

Keywords:
Complexation
Ligand
Liposomes
Micelles
Photosensitization
Principal component analysis
Pyridine

ABSTRACT

Photophysical and singlet oxygen ($^1O_2$) sensitization processes of Mg-tetrabenzoporphyrin (MgTBP) were studied upon complexation of the central Mg ion with pyridine. The addition of pyridine affected the absorption spectrum of MgTBP due to complexation, shifting the Soret absorption peak by as much as 13 nm. Principal component analysis (PCA) was employed to resolve the spectrum of MgTBP from the mono-ligand and bi-ligand complexes, MgTBP(pyr)$_1$ and MgTBP(pyr)$_2$, respectively. We found that the quantum yield of singlet oxygen production (Φ_Δ) by MgTBP was also affected by complexation of pyridine. In chloroform, toluene, water and SDS micelles the bi-ligand complexes had a higher quantum yield than MgTBP, by as much as 70%. In those solvents in which the mono-liganded complex was isolated, we found that its singlet oxygen quantum yield was higher than that of MgTBP by up to 20%. This enhancement can be explained by a relatively more efficient intersystem crossing of the complexes. We also found that MgTBP is capable of intercalating into a non-polar microenvironment of SDS micelles or lecithin liposomes. The axial pyridine ligands were, however, shed-off when the molecule entered the lipid bilayer of liposomes while they remained complexed when entering the micelle environment. This probably arises from the tight and ordered liposomal lipid phase as compared with the more fluid micellar environment.

1. Introduction

Metalloporphyrins have been extensively studied for many years because of their biological, catalytic and photophysical properties [1–3]. Magnesium porphyrins represent a particularly important class of metalloporphyrin compounds because of their relevance to the structure of chlorophyll1 [4]. Numerous metalloporphyrins and metallophthalocyanines have been studied in the last two decades, mainly for their photosensitizing capability, based on their efficient production of molecular singlet oxygen ($^1\Delta_g$).

One of the earliest metalloporphyrins to be studied was tetrabenzoporphyrin (TBP) and its Mg and Zn complexes, shown in Fig. 1 complexed with pyridine. Their complete synthesis was done by Linstead almost 70 years ago [5,6]. These molecules possess very strong and sharp absorption bands, which closely overlap common laser lines. Therefore they were considered as potential photosensitizers for biological and clinical applications [7]. The spectroscopic, photophysical, photochemical and photobiological attributes of the TBPs were studied and reported [8–11]. The axial coordination of nucleophilic ligands on the central ion is a typical and characteristic property of metal complexes of porphyrins with planar structure [12,13]. Mg-tetrabenzoporphyrin (MgTBP) is known to be capable of binding pyridine molecules as ligands and form such complexes [8,14]. Cromer et al. have investigated the reaction of pyridine with a series of metallo-tetrabenzoporphyrins (MTBP, where M = Cd(II), Zn(II), VO(IV), Cu(II), Mg(II), and Ni(II)). They discovered that only NiTBP in DMF and MgTBP in benzene bound two pyridine ligands with apparently different equilibrium constants [15]. A similar molecule, bis(pyridine)-(5,10,15,20-tetraphenylporphyrinato) magnesium(II), was studied by solid state ^{25}Mg NMR, X-ray crystallography and quantum mechanical calculation [16]. This study reported that the central Mg ion in this molecule is coordinated to four pyrrole nitrogen atoms and two nitrogen atoms from the axial pyridine ligands, forming a regular octahedron.

In this manuscript we report our studies on the binding of pyridine to MgTBP and the stoichiometry of the complexation. We employed principal component analysis (PCA) to resolve, globally, the spectra of the various species. We describe the effect of pyridine complexation on the absorption and fluorescence spectra and on the efficiency of photosensitized generation of singlet oxygen. We also describe a major difference in the entry of the pyridine complex of MgTBP into non-polar microenvironments, namely SDS micelles and lecithin liposomes.

* Corresponding author at: Department of Physics, Bar Ilan University, Ramat Gan 52900, Israel. Tel.: +972 3 5318427; fax: +972 3 7384054.
E-mail address: ehren@mail.biu.ac.il (B. Ehrenberg).
[1] BE is the incumbent of the Falk Chair in Laser Phototherapy.

1010-6030/$ – see front matter © 2009 Elsevier B.V. All rights reserved.
doi:10.1016/j.jphotochem.2008.11.026

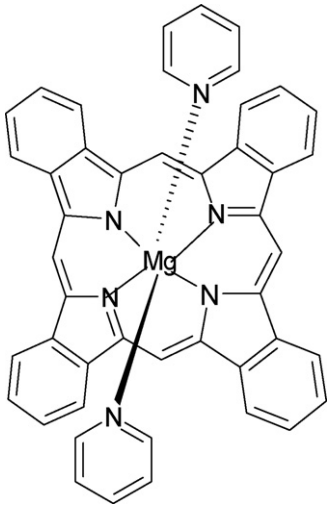

Fig. 1. Chemical structure of Mg(II)-tetrabenzoporphyrin bipyridine complex, MgTBP(pyr)$_2$.

2. Experimental

2.1. Materials

Mg^{2+}-tetrabenzoporphyrin (MgTBP) was prepared according to Barrett and Linstead [5,6]. To ensure its purity, the final step in the organic synthesis was sublimation of the compound at 450–500 °C. The chemical formula $C_{36}H_{20}MgN_4$, was confirmed by high resolution mass spectrometry. Acetone, dioxane, dimethyl formamide (DMF), ethanol, tetrahydrofuran (THF) and toluene were obtained from Bio Lab Ltd. (Jerusalem, Israel). Benzene, dimethyl sulfoxide (DMSO), pyridine (spectroscopic grade), and sodium dodecyl sulfate (SDS) were from Merck Chemicals Ltd. (Darmstadt, Germany). Chloroform and diethyl ether were obtained from Frutarom Ltd. (Haifa, Israel). 9,10-Dimethylanthracene (DMA), formamide, methylene blue (MB), L-α-phosphtidylcholine (PC, L-α-lecithin) type XIII-E from egg yolk (99%, 100 mg per ml ethanol) and 5,10,15,20-tetraphenyl 21H, 23H-porphine (99%) (TPP) were from Aldrich Chemical Company Inc. (St. Louis, MO, USA). Organic solvents were of analytical purity. Water was doubly distilled. Stock solutions of MgTBP and DMA were prepared in DMSO, at 1 mM, and in DMF, at 2 mM, respectively. The spectroscopic measurements were carried out at a concentration of 1–3 μM MgTBP and 3–5 μM DMA.

2.2. Preparation of liposomes

The lipid was layered at the bottom of a vial by evaporating the ethanol under a stream of nitrogen. Diethyl ether was added and the solution was thoroughly re-evaporated to complete dryness. Water was added to the dried lipid to form lipid concentration of, usually, 5 mg/ml. The sample was vortexed for 3 min and then sonicated for 20 min, at 4 °C, by a probe sonicator (Sanyo-MSE, Crawley, UK) until a clear sample was obtained. This was the stock suspension of unilamellar liposomes, as confirmed by electron microscopy.

2.3. General analytical and instrumental techniques

Absorption spectra were measured on a Shimadzu (Kyoto, Japan) UV-2501PC UV–vis spectrophotometer. Fluorescence spectra and time-drive traces of fluorescence intensity were recorded on a Perkin Elmer (Norwalk, CT) LS-50B fluorimeter, controlled by FL-WinLab software.

2.4. Evaluation of coordination constants of pyridine to MgTBP

The binding constants for the two steps of pyridine coordination to TBP, K_1 and K_2, were evaluated from spectroscopic measurement of MgTBP in various solvents (at 1–1.5 μM), while it was titrated with pyridine. At the end of titration the pyridine volume fraction did not exceed 5%.

Since the absorption spectrum of MgTBP partially overlaps the spectrum of the molecule with pyridine complexation, we had to resolve the absorption spectra of the different species. This was done on a large set of spectra acquired along the titration, by global analysis, using PCA [17]. PCA involves a mathematical procedure that transforms a set of correlated variables into a smaller set of uncorrelated variables called principal components, which are ordered by reducing variability. The uncorrelated variables are linear combinations of the original variables. The main use of PCA is to reduce the dimensionality of a data set while retaining as much information as is possible. The first principal component accounts for as much of the variability in the data as possible, and each succeeding component accounts for as much of the remaining variability as possible. All principal components are independent of each other. PCA is carried out under MATLAB (The MathWorks, Natick, MA, USA) environment. The procedure thus results, in our studied cases, in three eigen spectra, namely the spectrum of MgTBP, MgTBP(pyr)$_1$ and MgTBP(pyr)$_2$ as well as the contribution of each of them to every one of the spectra that were measured and analyzed. These contributions are the relative fractions of the three components that were in equilibrium at every pyridine concentration. We thus obtain the true concentrations of MgTBP, MgTBP(pyr)$_1$ and MgTBP(pyr)$_2$ in each of the measured spectra. These concentrations were used to calculate K_1 and K_2, the association constants of the first and second pyridine ligand, respectively.

2.5. Singlet oxygen quantum yield (Φ_Δ) measurements

The Φ_Δ values were determined in four solvents: chloroform, toluene, water and SDS micelles, all without and with certain concentrations of pyridine. The 632.8 nm HeNe laser line was used for the illumination of MgTBP and its pyridine complexes, MgTBP(Pyr)$_n$. The laser beam transversed the sample cuvette along its long axis, at 90° to the direction of the excitation and emission channels of the fluorimeter, in which the cuvette was placed. The intensity of the beam near the sample's surface (~15 mW) was measured with a laser power meter (model PD2-A, Ophir, Jerusalem, Israel), before and after the measurements, to ensure that the power remained constant during the measurement. The sample was air-saturated and stirred magnetically to obtain uniform illumination of the whole sample.

The attributes of the samples for the photophysical measurements were as follows. The volume of the illuminated sample was 3 ml. The singlet-oxygen target DMA (at 3 μM) was employed, since it reacts selectively and rapidly with singlet oxygen ($^1O_2$) to form an endoperoxide ($DMAO_2$) and because it can be followed easily by its fluorescence, which is not affected by spectral properties of the sensitizers [18]. The fluorescence of DMA was excited near 360 nm, at a wavelength where the absorbance was <0.05 optical density units. Under such conditions the fluorescence intensity, which is monitored at 455 nm, is proportional to DMA concentration. DMA's diminishing fluorescence intensity, which is monitored in a time-drive mode, can thus be considered to reflect its disappearance as a result of the photosensitization reaction. The fluorimeter has a pulsed light source with phase-sensitive detection electronics. These properties are important as they serve to reject any stray light from the illuminating laser beam. Its presence, even at high intensity, does not interfere with the measurement of the fluorescence of DMA.

The production rate of excited photosensitizer molecules, in molar concentration units per second, k_{pho}, is given by the following equation [19]:

$$k_{pho} = \frac{0.98\ P(1 - 10^{(-abs\,L)})}{EV} \quad (1)$$

where P is the laser power (in mW), *abs* is the optical density per cm of the photosensitizer at the laser's wavelength, L is the length of the laser beam path along the sample (in cm), E is the number of Einstein units (1 Einstein = 6.023×10^{23} photons) of light energy per second per watt of light at the illumination wavelength and V is the sample's volume (in ml). The factor 0.98 corrects for light reflection at the air/sample interface.

The time-drive traces of diminishing fluorescence intensity of DMA were fitted to exponential decays (Eq. (2)) by least-squares fitting (Origin, Microcal Software, Northampton, MA).

$$DMA_{flu} = Ae^{-k_{DMA}\ time} \quad (2)$$

where k_{DMA} is the rate constant for the disappearance of DMA's fluorescence intensity, DMA_{flu}. $\Phi_{\Delta,MgTBP(pyr)_n}$ is proportional to the singlet oxygen quantum yield of $MgTBP(pyr)_n$. ($MgTBP(pyr)_0$ = MgTBP) and is expressed by Eq. (3).

$$\Phi_{\Delta,MgTBP(pyr)_n} \propto \left(\frac{k_{DMA}}{k_{pho}}\right)_{MgTBP(pyr)_n} \quad (3)$$

The singlet oxygen quantum yield, Φ_Δ, of $MgTBP(Pyr)_n$ was measured and calculated by Eq. (4). The destruction of DMA by photosensitization with the studied MgTBP species was carried out in the same solvents as with a standard sensitizer. As standards for measurements in chloroform and toluene we used TPP, and for water and micelles we used MB. The reported singlet oxygen yields of TPP in chloroform and in toluene are 0.52 and 0.79, respectively and for MB in water and micelles are 0.50 and 0.37, respectively [20].

$$\frac{\Phi_{\Delta,MgTBP(pyr)_n}}{\Phi_{\Delta,ref}} = \frac{(k_{DMA}/k_{pho})_{MgTBP(pyr)_n}}{(k_{DMA}/k_{pho})_{ref}} \quad (4)$$

2.6. Estimates of the mean and error for Φ_Δ and for the coordination constants K_1 and K_2

The values of Φ_Δ and K were determined by a statistical average of two or three independent, repeated measurements, based on the equations below. The average, μ, of several measurements, each yielding a result x_i and a measurement error σ_i, is calculated by Eq. (5) [21]:

$$\mu \cong \frac{\sum(x_i/\sigma_i^2)}{\sum(1/\sigma_i^2)}, \quad \sigma_\mu^2 \cong \frac{1}{\sum(1/\sigma_i^2)} \quad (5)$$

The uncertainty of this calculated average, σ_μ, is also given in Eq. (5) [21].

3. Results and discussion

3.1. Absorption and fluorescence spectra

The symmetric structure of MgTBP possesses D_{4h} symmetry and therefore has full in-plane symmetry, which degenerates the X and Y electronic transitions [22,23]. The effect of pyridine coordination with MgTBP on its absorption spectrum was investigated in 11 solvents. The locations of the main Soret bands of MgTBP, before and after coordination with pyridine, are listed in Table 1. In some solvents (dimethylformamide, dioxane, ethanol, formamide and tetrahydrofuran) the location of the Soret band of MgTBP was at 431–435 nm, and it exhibited a small red-shift, by only 1–3 nm, upon addition of pyridine. In contrast, in acetone, benzene, chloroform, diethylether, SDS micelles, toluene and water, the location of the Soret band red-shifted significantly after full complexation with pyridine, by 12–13 nm, from 423–429 nm to 436–441 nm.

It is important to notice that since the maximum pyridine content in all the solvents was 5% (v/v), the spectral shifts reflect the effect of coordination of pyridine rather than its solvatochromic effect. Such solvatochromic effect is revealed only upon increasing the pyridine content to almost neat pyridine, in which the Soret band is shifted further to 442 nm, reflecting the absorption spectrum of $MgTBP(pyr)_2$ in pyridine (see later). As with other porphyrins, the location of the Q bands is much less sensitive to the nature of the solvent or to complexation of pyridine. As can be seen in Table 1, the location of the Q band differs by only 3 nm between the abovementioned solvents (627–630 nm) and the addition of pyridine broadens the band slightly and red shifts it by only 1–3 nm, as can be seen in Fig. 2.

3.2. Coordination constants of MgTBP with pyridine

The coordination state of MgTBP with pyridine affects the absorption spectrum, namely the number, location and intensity of the bands. The changes in the Soret region in a set of absorption spectra of MgTBP in chloroform and toluene, that was titrated stepwise with pyridine, was inspected and the results were analyzed as was done previously by Cromer et al. in benzene [15] and by Ehrenberg and Johnson in benzene, decane and ethanol [8]. However, in those studies the absorbance at a single specific wavelength in the Soret region was traced, while in the present study we monitored the whole Soret spectral region, using PCA [17,24]. We have employed this methodology in a previous study of fluorinated phthalocyanines [19]. PCA provides the minimal number and the shape of the basic spectra, which comprise, by

Table 1
Location of the Soret and Q bands of MgTBP before and after coordination with pyridine. n = 1 or 2 is based on the assumption that a large spectral shift, >10 nm, is an indication of coordination of 2 pyridine molecules, while a shift of 1–3 nm indicates coordination of one molecule.

solvent	MgTBP absorption peaks (nm) (extinction coefficients × 10^4) ($M^{-1}\,cm^{-1}$)		$MgTBP(pyr)_n$ absorption peaks (nm) (n = 1 or 2)		
Acetone	424(32)	627(9.1)	436	630	(2)
Benzene	429(32)	630(10)	440	632	(2)
Chloroform	428(30)	630(8.4)	440	632	(2)
Diethyl ether	423(51)	626(14)	436	629	(2)
Dimethylformamide	434(26)	628(0.8)	436	629	(2)
Dioxane	430(29)	627(6.4)	433	628	(1)
Ethanol	431(28)	627(7.5)	433	628	(1)
Formamide	430(38)	633(6.6)	433	633	(1)
SDS micelles	425(13)	630(3.3)	439	632	(2)
Tetrahydrofuran	432(43)	627(9.3)	433	628	(1)
Toluene	429(35)	627(11)	441	630	(2)
Water	429(0.8)	630(0.6)	439	631	(2)

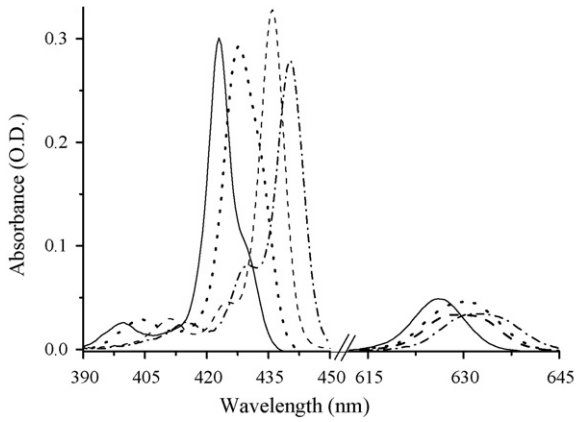

Fig. 2. Absorption spectra of 1 μM MgTBP (solid line) and MgTBP(pyr)$_2$ (dashed line) in diethylether and spectra of 1 μM MgTBP (dotted line) and MgTBP(pyr)$_2$ (dashed dotted line) in chloroform.

their linear combinations, all the measured spectra. It also yields the concentration fractions of these basic species in each case. Thus, PCA of a whole set of absorption spectra of MgTBP with increasing concentrations of pyridine deconvolutes the spectra of MgTBP, MgTBP(pyr)$_1$ and MgTBP(pyr)$_2$ and provides the association constants of pyridine to MgTBP, given in Eq. (6):

$$\begin{aligned} &\mathrm{MgTBP} + \mathrm{pyridine} \overset{K_1}{\rightleftharpoons} \mathrm{MgTBP(pry)_1} \\ &\mathrm{MgTBP(pry)_1} + \mathrm{pyridine} \overset{K_2}{\rightleftharpoons} \mathrm{MgTBP(pry)_2} \end{aligned} \tag{6}$$

We chose to study the complexation constants of pyridine to MgTBP by PCA, in chloroform and toluene, in which this complexation leads to a large spectral change as a model to other solvents that showed a similar phenomenon, namely red shifted by 10–14 nm. MgTBP (1 μM) was titrated in these two solvents with pyridine, up to pyridine concentration of 0.5 M (~5% by volume). As an example, some of the spectra that were measured in toluene are shown in Fig. 3A (solid lines). As can be seen, the Soret band shifted to longer wavelength upon titration with pyridine, as was explained above. Resolution of the spectra by PCA revealed, however, that besides the basic component spectra with peaks at 428 nm, of MgTBP, and at 441 nm, of MgTBP(pyr)$_2$, another band is observed at 438 nm (Fig. 3A). The existence of a third species can be anticipated from the lack of a clear isosbestic point, which would have implied two components only. Fig. 3B shows the calculated fractions of the three resolved components, at different concentrations of added pyridine. As can be seen in this graph, the concentration of MgTBP vanishes already at a pyridine concentration of 3 mM while the concentration of the species with the 438 nm band increases concomitantly. This indicates that this band belongs to MgTBP(pyr)$_1$. Further increase in pyridine's concentration leads to a gradual, slow, decrease in this species' concentration with a concurrent increase in the concentration of MgTBP(pyr)$_2$. As can be seen in Fig. 3B, at 0.14 M pyridine, MgTBP(pyr)$_2$ is almost the only species that exists. Its extinction coefficient in toluene is $3.50 \times 10^5\ \mathrm{M^{-1}\,cm^{-1}}$ at 441 nm and $0.76 \times 10^5\ \mathrm{M^{-1}\,cm^{-1}}$ at 630 nm.

A similar two-step process was observed on titration of MgTBP with pyridine in chloroform. The spectrum is only slightly red shifted from 428 nm for MgTBP to 430 nm for MgTBP(pyr)$_1$ and then further to 440 nm, for MgTBP(pyr)$_2$. Its extinction coefficients in chloroform are $5.37 \times 10^5\ \mathrm{M^{-1}\,cm^{-1}}$ at 440 nm and $1.02 \times 10^5\ \mathrm{M^{-1}\,cm^{-1}}$ at 632 nm. It is possible that the small initial red shift (2 nm) upon formation of the MgTBP(pyr)$_1$ complex in chloroform, *vs.* the larger shift (10 nm) in toluene, arises from solvatochromic effects [25]. Polar chloroform apparently stabilizes, by solvation, the ground state of the polar MgTBP(pyr)$_1$ species better than does non-polar toluene. Therefore the excitation energy that is required in chloroform is larger than in toluene. It is worth noticing that molecular orbital calculations have shown that in Mg-porphyrins that are mono-liganded by pyridine, the Mg atom seems to come off the plane of the porphyrin ring, while in six coordinated molecules, with two axial pyridines the Mg atom appears to be back in the center of the planar porphyrin ring [26].

The concentrations of the three basic components were used to calculate the equilibrium constants of the pyridine binding reactions, shown in Eq. (6). The constants are given in Table 2. As can be seen in this Table, the complexation of the first pyridine axial ligand is strongly favored, having a very high binding constant. The high constant in toluene means, for example, that already at 100 μM pyridine about 90% of MgTBP exists as the MgTBP(pyr)$_1$ species.

Our calculated coordination constants of MgTBP, K_1 and K_2, differ from each other by ~3 orders of magnitude, in toluene and in

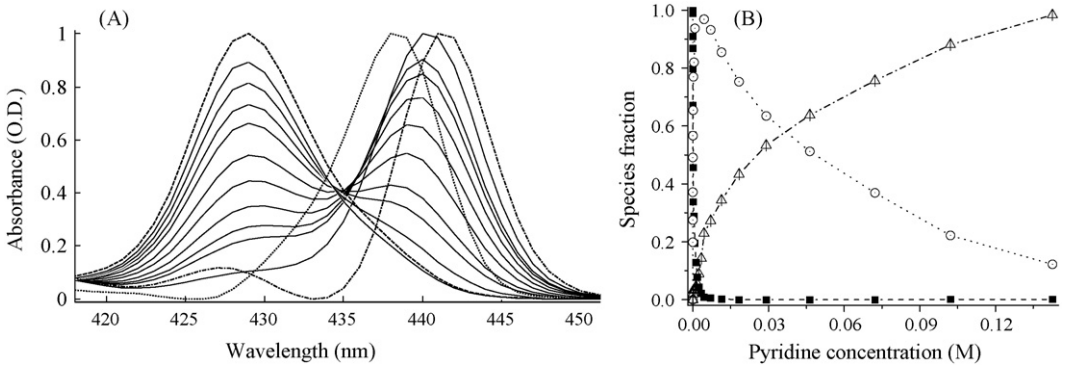

Fig. 3. (A) Absorption spectra of 1 μM MgTBP in toluene at increasing pyridine concentrations up to 0.5 M (solid lines) and normalized spectra of MgTBP (dashed line), MgTBP(pyr)$_1$ (dotted line) and MgTBP(pyr)$_2$ (dashed dotted line) that were resolved by PCA. (B) Calculated fractions of the three species at equilibrium, as a function of pyridine concentration. MgTBP (filled black squares), MgTBP(pyr)$_1$ (empty circles) and MgTBP(pyr)$_2$ (empty triangles).

Table 2
The location of the Soret band peaks of the three MgTBP species and equilibrium constants for the coordination reactions of pyridine, in chloroform and toluene.

Solvent	MgTBP Soret band (nm)	K_1 ($\mathrm{M^{-1}}$)	MgTBP(pyr)$_1$ Soret band (nm)	K_2 ($\mathrm{M^{-1}}$)	MgTBP(pyr)$_2$ Soret band (nm)
Chloroform	428	38000 ± 259	430	6.0 ± 0.2	440
Toluene	429	76000 ± 2880	438	145.0 ± 2.5	441

Table 3
Singlet oxygen quantum yield, Φ_Δ, of MgTBP, MgTBP(pyr)$_1$ and MgTBP(pyr)$_2$ in chloroform, toluene, water and SDS micelles.

Solvent	$\Phi_{\Delta,\mathrm{MgTBP}}$	$\Phi_{\Delta,\mathrm{MgTBP(pyr)_1}}$	$\frac{\Phi_{\Delta,\mathrm{MgTBP(pyr)_1}}}{\Phi_{\Delta,\mathrm{MgTBP}}}$	$\Phi_{\Delta,\mathrm{MgTBP(pyr)_2}}$	$\frac{\Phi_{\Delta,\mathrm{MgTBP(pyr)_2}}}{\Phi_{\Delta,\mathrm{MgTBP}}}$
Chloroform	0.47 ± 0.01	0.58 ± 0.01	1.24 ± 0.05	0.80 ± 0.01	1.7 ± 0.3
Toluene	0.15 ± 0.01	0.17 ± 0.01	1.10 ± 0.10	0.21 ± 0.02	1.4 ± 0.1
Water	0.69 ± 0.10			1.10 ± 0.20	1.6 ± 0.4
SDS micelles	0.19 ± 0.01			0.24 ± 0.01	1.3 ± 0.1

chloroform. These results are consistent with the results of Ehrenberg and Johnson in benzene [8]. Interestingly, an early study has reported that the magnesium complexes of similar molecules, tetraphenylporphine and tetraphenylchlorin, form dipyridinate complexes, while other metal cations form only monopyridine complexes [27]. This report has also estimated the first binding constant, K_1, to be 2000–4000 M^{-1} and K_2 as 0.5–0.9 M^{-1}, both about 10 times lower that our measured binding constants for MgTBP. Yamauchi et al. have demonstrated for one of the abovementioned molecules, MgTPP, that the binding constant of the second pyridine ligand, K_2, is much higher in the S_1 excited state than in the ground state, 8.5 M^{-1} vs. 0.65 M^{-1} [28].

Satake and Kobuke showed in their review that the solvent has a dramatic effect on the binding constant of a pyridine to ZnTPP [29]. We assume that in the solvents in which the red shift by pyridine was 12–13 nm (acetone, benzene, diethyl ether and SDS micelles) there are also 2 coordination states similar to those in chloroform and toluene. Similarly, we assume that in the solvents in which the red shift was only 1–3 nm, namely DMF, dioxane, ethanol, formamide and THF, only mono-coordination with pyridine exists, as was shown previously in ethanol [8]. In such solvents there is a possibility of mixed complexes, namely pyridine-Mg-solvent. Such species have been shown to exist in some porphyrin iron(II) complexes [30]. This can explain the fact that only one-step of pyridine coordination is observed in these solvents and, as a result, the small spectral shift.

3.3. Singlet oxygen quantum yield of MgTBP(pyr)$_n$ species

There is a growing interest in developing photosensitizers which are more efficient than the known first- and second-generation sensitizers. MgTBP has the advantage of possessing very strong absorption bands and was indeed found to photosensitize the photodamaging of bacterial and animal cells [7]. In the present study we were interested in the effect of pyridine complexation on the production efficiency of singlet oxygen as a model to other biological systems. We measured the singlet oxygen yields of MgTBP, MgTBP(pyr)$_1$ and MgTBP(pyr)$_2$ in a few solvents. The yield of intermediate MgTBP(pyr)$_1$ was evaluated after adding 0.003 M and 0.008 M pyridine in toluene and chloroform, respectively. At these concentrations PCA analysis has indicated that the composition of the three species in equilibrium, namely MgTBP, MgTBP(pyr)$_1$ and MgTBP(pyr)$_2$ was 1:87:12 in chloroform and in toluene, thus the monocomplex MgTBP(pyr)$_1$ was at optimal concentration. To measure the yield of MgTBP(pyr)$_2$ we added 0.5 M pyridine (~5%, v/v pyridine/solvent). At this concentration the major species is (more than 98%) MgTBP(pyr)$_2$. As can be seen from the quantum yields in Table 3, coordination with pyridine increases significantly the singlet oxygen quantum yield of the complex in comparison to that of bare MgTBP, in the same solvents. The relative enhancement of singlet oxygen quantum yield by MgTBP(pyr)$_n$ is between 10%, in toluene for MgTBP(pyr)$_1$, up to 70% in chloroform for MgTBP(pyr)$_2$. In these two solvents it is evident that MgTBP(pyr)$_1$ is also a better producer of singlet oxygen than ligand-free MgTBP.

This study appears to be the first indication that the axial ligand affects the photosensitizing capacity of a sensitizer molecule. MgTBP(pyr)$_2$ can be a potential photosensitizer for PDT, based on its good efficiency. This complex can serve as a model for other metalloporphyrins that could be chelated by coordination with an organic base, such as the amino acid histidine. The effect of such complexation should be tested as a means of enhancing the photosensitized killing of cancer and bacterial cells.

3.4. Partitioning of MgTBP and its pyridine complex into microenvironments

We studied the binding of MgTBP and MgTBP(pyr)$_2$ to unilamellar liposomes. A sample of 1.3 μM MgTBP in water, and another sample that contained 1.3 μM MgTBP and 0.9 mM pyridine in water, conditions that favor the formation of MgTBP(pyr)$_2$, were dispersed in a suspension of lipid, at a relatively high concentration of 1 mg/ml. At these low concentrations, the absorbance of MgTBP was linear with concentration, thus showing no signs of aggregation. The sample was left over night on a shaker. Both samples exhibited at the end identical absorption spectra, with the major bands at 429 and 629 nm. The spectrum differed from the original spectrum in water in the intensity and width of the ~429 nm band and in the relative intensity and location of the band around 410 nm. In addition, when pyridine was added (up to 5% volume) to the sample containing MgTBP in liposomes, no spectral change was observed. We conclude that MgTBP enters the lipid phase, but MgTBP(pyr)$_2$ does not penetrate into it and it does not form in the lipid phase. In order to clarify the reason for MgTBP shedding off its axial pyridine ligands when partitioning into lipid bilayer we studied its partitioning into micelles. Micelles composed of sodium dodecyl sulphate (SDS) are used extensively as a model to investigate the effect of heterogeneous environments and microenvironment on photophysical properties of photosensitizers. We measured the absorption spectra of MgTBP and MgTBP(pyr)$_n$ in water solution containing SDS at a concentration of 20 mM, higher than the critical micelles concentration in water, 8 mM [31,32]. The absorption spectrum of MgTBP shifts, from 429 nm, its peak location in water, to 425 nm, when SDS micelles are added. When SDS is added into an aqueous solution of MgTBP(pyr)$_2$, or when pyridine is added to MgTBP in SDS micelles, the Soret spectral peak red-shifts to 439 nm. Thus, the pyridine complex of MgTBP does partition into the micellar microenvironment. We attribute its lack of solubility in a lipid bilayer membrane of liposomes to a steric hindrance which precludes proper intercalation of this bulky molecule in the tight, highly ordered, lipid bilayer. The equilibrium that exists between the pyridine complex and pyridine-free MgTBP thus shifts the equilibrium, in the presence of liposomes, to the formation of free MgTBP, which is taken up by the lipid phase.

4. Conclusion

We report the strong effects of complexation of pyridine to MgTBP on the electronic absorption spectrum, on singlet oxygen quantum yield and on partitioning into amphiphilic microenvironments. A significant enhancement of singlet oxygen quantum yields of MgTBP(pyr)$_2$ and MgTBP(pyr)$_1$, in comparison to MgTBP, was observed. We also show that the coordination constant of the first pyridine is approximately three orders of magnitude higher than for the second pyridine coordination, in chloroform and toluene.

Acknowledgments

We thank Prof. Fred M. Johnson, from the Dept. of Physics at California State University at Fullerton for supplying us with MgTBP. We would like to acknowledge the support of the Michael David Falk Chair in Laser Phototherapy to B.E.

References

[1] K.M. Kadish, K.M. Smith, R. Guilard, The Porphyrin Handbook, Academic Press, Burlington, MA, 1999.
[2] L.R. Milgrom, The Colours of Life: An Introduction to the Chemistry of Porphyrins and Related Compounds, Oxford University Press, New York, 1997.
[3] K.M. Smith, Porphyrins and Metalloporphyrins, Elsevier, Amsterdam, 1975.
[4] H. Scheer, Chlorophylls, CRC Press, Boca Raton, FL, 1991.
[5] R.P. Barrett, R.P. Linstead, F.G. Rundall, G.A.D. Tuey, Phtalocyanines and related compounds. XIX. Tetrabenzoporphyrin, tetrabenzmonazaporphyrin and their metallic derivatives, J. Chem. Soc. 92 (1940), 1097–1092.
[6] P. Linstead, Discoveries among conjugated macrocyclic compounds, J. Chem. Soc. 105 (1953) 2873–2884.
[7] B. Ehrenberg, Z. Malik, Y. Nitzan, H. Ladan, F.M. Johnson, J.L. Sessler, The binding and photosensitization of tetrabenzoporphyrins and texaphyrin in bacterial and leukemic cells, Lasers Med. Sci. 8 (1993) 197–203.
[8] B. Ehrenberg, F.M. Johnson, Spectroscopic studies of tetrabenzoporphyrins: MgTBP, ZnTBP and H_2 TBP, Spectrochim. Acta 46A (10) (1990) 1521–1532.
[9] M.R. Lee, S.T. Liou, R.J. Cheng, Study of adduct ions of meso-phenyl-substituted tetrabenzoporphyrins by fast-atom bombardment mass spectrometry, J. Am. Soc. Mass. Spectrom. 8 (1997) 62–67.
[10] Y. Matsuzawa, K. Ichimura, K. Kudo, Preperation of soluble tetrabenzoporphyrins with substituents at the peripheral positions, Inorg. Chim. Acta 277 (1997) 151–156.
[11] H. Stiel, A. Volkmer, I. Ruckmann, A. Zeug, B. Ehrenberg, B. Röder, Non-linear and transient absorption spectroscopy of magnesium (II)-tetrabenzoporphyrin in solution, Opt. Commun. 155 (1998) 135–143.
[12] J.W. Buchler, Static coordination chemistry of metalloporphyrins, in: K.M. Smith (Ed.), Porphyrins and Metalloporphyrins, Elsevier, Amsterdam, 1975, pp. 157–231.
[13] H. Scheer, J.J. Katz, Nuclear magnetic resonance spectroscopy of porphyrins and metalloporphyrins, in: K.M. Smith (Ed.), Porphyrins and Metalloporphyrins, Elsevier, Amsterdam, 1975, pp. 399–452.
[14] P. Hambright, Dynamic coordination chemistry of metalloporphyrins, in: K.M. Smith (Ed.), Porphyrins and Metalloporphyrins, Elsevier, Amsterdam, 1975, pp. 233–278.
[15] S. Cromer, P. Hambright, J. Grodkowski, P. Neta, Tetrabenzoporphyrins: metal incorporation and exchange kinetics, ligational equilibria and pulse radiolysis studies, J. Porphyr. Phthal. 1 (1997) 45–54.
[16] W. Gang, A. Wong, W. Suning, Solid state ^{25}Mg NMR, X-ray crystallographic, and quantum mechanical study of bis(pyridine)-(5,10,15,20-tetraphenylporphyrinato) magnesium(II), Can. J. Chem. 81 (2003) 275–283.
[17] E.R. Malinowski, Factor Analysis in Chemistry, Wiley-Interscience Publication, New York, 1991.
[18] E.A. Lissi, M.V. Encinas, E. Lemp, M.A. Rubio, Singlet oxygen O_2(1.DELTA. g) bimolecular processes. Solvent and compartmentalization effects, Bol. Soc. Chil. Quim. 93 (1993) 699–723.
[19] H. Weitman, S. Schatz, H.E. Gottlieb, N. Kobayashi, B. Ehrenberg, Spectroscopic probing of the acid–base properties and photosensitization of afluorinated phthalocyanine in organic solutions and liposomes, Photochem. Photobiol. 73 (2001) 473–481.
[20] F. Wilkinson, W.P. Helman, A.B. Ross, Quantum yields for the photosensitized formation of the lowest electronically excited singlet state of molecular oxygen in solution, J. Phys. Chem. Ref. Data 22 (1993) 113–262.
[21] P.R. Bevington, Data Reduction and Error Analysis for the Physical Sciences, McGraw-Hill, New York, 1969.
[22] M. Gouterman, Optical spectra and electronic structure of porphyrins and related rings, in: D. Dolphin (Ed.), The Porphyrins, vol. III, Academic Press, 1978, pp. 1–165.
[23] M. Gouterman, Spectra of porphyrins, J. Mol. Spectrosc. 6 (1961) 138–163.
[24] D.E. Irish, T. Ozeki, Raman spectroscopy of inorganic species in solution, in: J.G. Grasselli, B.J. Bulkin (Eds.), Analytical Raman spectroscopy, Wiley, New York, 1991, pp. 59–106.
[25] C. Reichardt, Solvents and Solvents Effects in Organic Chemistry, second ed., VCH, Weinheim, 1990.
[26] J. Linnanto, J. Korppi-Tommola, Semiempirical PM5 molecular orbital study on chlorophylls and bacteriochlorophylls: comparison of semiempirical, ab initio, and density functional results, J. Comput. Chem. 25 (2003) 123–137.
[27] J.R. Miller, G.D. Dorough, Pyridinatedcomplexes of some metallo-derivatives of tetraphenylporphine and tetraphenylchlorin, J. Am. Chem. Soc. 74 (1952) 3977–3981.
[28] S. Yamauchi, Y. Suzuki, T. Ueda, K. Akiyama, Y. Ohba, M. Iwaizumi, Fluorescence studies on the photoinduced ligation in the excited singlet-state of magnesium tetraphenylporphine, Chem. Phys. Lett. 232 (1995) 121–126.
[29] A. Satake, Y. Kobuke, Dynamic supramolecular porphyrin systems, Tetrahedron 61 (2005) 13–41.
[30] N.S. Lebedeva, S.P. Yakubov, A.I. Vyugin, E.V. Parfenyuk, Termodynamics of complex formation of natural iron(III)porphyrins with neutral ligands, Thermochim. Acta 404 (2003) 19–24.
[31] P.J. Missel, N.A. Mazer, G.B. Benedek, C.Y. Young, M. Carey, Thermodynamic analysis of the growth of sodium dodecyl sulfate micelles, J. Phys. Chem. 84 (1980) 1044–1057.
[32] A. Helenius, D.R. McCaslin, E. Fries, C. Tanford, Properties of detergents, Meth. Enzymol. 56 (1979) 734–749.